An Analysis of the Thermal Motion in the Negative Thermal Expansion Material $Sc_2(WO_4)_3$ Using Isotopes in Neutron Diffraction

Mark T. Weller,*,† Paul F. Henry,† and Chick C. Wilson‡

Department of Chemistry, University of Southampton, Southampton SO17 1BJ, U.K., and Rutherford-Appleton Laboratory, Chilton, Didcot, Oxford OX11 0QX

Received: August 22, 2000; In Final Form: September 28, 2000

A full analysis of thermal motion has been carried out for the negative thermal expansion material $Sc_2(WO_4)_3$ over the temperature range 50−823 K. By obtaining neutron diffraction data from isotopically pure samples of the compositions $Sc_2(^{184}WO_4)_3$, $Sc_2(^{186}WO_4)_3$ and natural $Sc_2(WO_4)_3$, coupled with multidata set refinement methods, it is possible to extract anisotropic thermal parameters for individual atoms throughout the temperature range. Results indicate that the thermal motion of two Sc−O−W bridging oxygen atoms with the largest Sc−O−W angles is better represented by thermal toroids consistent with strong local motion of these units. The thermal behavior of the other oxygen atoms in the structures as a function of temperature is normal. Sc−O and W−O bond lengths corrected for the effect of correlated thermal motion show the expected increase with temperature.

Introduction

Research on negative thermal expansion (NTE) materials has recently undergone a renaissance with the discovery and investigation of new polyhedral structures that exhibit this effect. Materials which have been studied in detail include materials of the type $M_2(XO_4)_3$,[1,2] ZrW_2O_8,[3] β-quartz,[4,5] $Sr_{0.5}Ti_2(PO_4)_3$,[6] $NbOPO_4$,[7] and a number of zeolite materials such as AlPO-17.[8] The structures and behaviors of many of these materials have recently been reviewed by Evans,[9] who also discusses the mechanistic origins of the lattice contractions that occur in these polyhedral materials. Dove et al.[10] have discussed in detail the behavior of negative thermal expansion materials in terms of modes involving the motion of rigid units.

Much of the effort has been focused on the structural investigations of these materials in an effort to find the origin of the behavior. The systems most intensively studied are ZrW_2O_8,[3,9] and materials of the composition $M_2(XO_4)_3$, M = Sc, Lu, Y, X = W, Mo.[1,2,11,12] Neutron diffraction studies of these materials have been used to describe changes in bond angles between the polyhedral centers which occur as a function of temperature. In essence, the origin of the contraction is believed to originate in coupled twisting or rocking of totally rigid polyhedra associated with the transverse vibrations of all the bridging oxygen atoms perpendicular to the M−O-X linkages, Figure 1. This is supported to some extent by theoretical analysis of the NTE effect in ZrW_2O_8 but this work recognizes the need to allow for some distortion of the polyhedra. The incorporation of the larger Lu into the $M_2(XO_4)_3$ structure, replacing Sc, results in a significant enhancement of the negative thermal expansion.[11] Work on $Y_2(WO_4)_3$, carried out over the temperature range 15−1373 K[12] clearly shows the need to consider the negative thermal expansion in terms of transverse oxygen motions rather than purely as an observed contraction of some M−O−W angles.

* Corresponding author. E-mail: mtw@soton.ac.uk. Fax: 00 44 23 80 593781.

† University of Southampton.

‡ Rutherford-Appleton Laboratory.

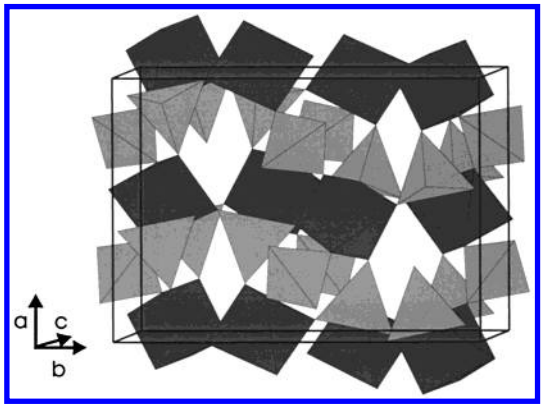

Figure 1. Polyhedral representation of the $Sc_2(WO_4)_3$ structure viewed down the *c* direction: ScO_6 octahedra, dark gray; WO_4, tetrahedra light gray.

The full, unconstrained, structural analysis of many of these NTE materials has been restricted by the complexity of their relatively low symmetry crystal structures. To obtain structural data relating to the oxygen positions and over a wide temperature range, powder neutron diffraction is the method of choice. The structural complexity, coupled with low scattering density from open frameworks, generally results in relatively poor data quality, with large numbers of overlapping, weak reflections − even on the best neutron diffraction instruments. Under these conditions powder diffraction methods often produce strong correlation between refined parameters unless additional constraints are used to limit the number of variables. In particular, the extraction of accurate thermal parameters, and specifically the anisotropic components, becomes very difficult, particularly from constant wavelength data with limited $\sin\theta/\lambda$, as accurate reflection intensities need to be obtained from a large *d* spacing range. Evans et al.[1] tried to overcome this problem with $Sc_2(WO_4)_3$ through the use of a rigid body model more normally applied to molecular units in crystal structures; such methods have been used successfully for the simple structure of β-quartz. While such rigid body methods can provide high quality and

10.1021/jp0030037 CCC: $19.00
Published on Web 12/02/2000

more precise extracted parameters than otherwise achievable with the data, the method is clearly unrealistic in terms of modeling certain aspects of the structure − for example the equivalent isotropic thermal parameters within the polyhedra all have to be equal despite atoms being in quite different environments. Such structural modeling seems reasonable for framework materials where all the bridging oxygen atoms have similar or identical environments, e.g., β-quartz, but are unlikely to be a good representation for materials with strongly varying types of oxygen. For example in $Sc_2(WO_4)_3$ the bridging oxygen bond angles vary over the range 145−172° and in ZrW_2O_8 from 140 to 172°.

This is not to say that interpretation of framework structures as rigid bodies—both in terms of structures and rigid unit modes—is incorrect but rather the assumptions made in such totally rigid descriptions; e.g., the bridging angle force constant is identical and zero for all sites, should be viewed with caution as the oxygen becomes less floppy—i.e., the bridging angle departs from 180°. In such cases quasi-rigid unit modes provide a better description of the vibrational motion and allow for small distortions of the polyhedra. However, quasi-rigid units cannot, as yet, be simply incorporated into a structure model as can rigid bodies.[10,12]

To extract better information on the motion of the bridging oxygen atoms in these materials, which is the origin of their unusual NTE behavior, it is clear that better quality neutron diffraction data is required to allow extraction of thermal parameters. Very high resolution structural data such as that available from instruments like HRPD (ISIS, RAL) and D2B (ILL, Grenoble), providing large well resolved data sets, potentially answer these problems but with the relatively low structural symmetry of $Sc_2(WO_4)_3$ deconvolution of various peak intensities and backgrounds at low *d* spacings remains a problem. High resolution diffractometers also generally produce weak sample scattering exacerbating problems inherent in studying framework materials, such as zeolites and NTE structures, leading to long experimental data collection times in order to produce good quality data at low *d* spacings.

We have recently identified one way of overcoming such problems with powder neutron data that involves the use of multiple samples of varying isotopic composition with good scattering contrasts between the isotopes. By using such samples and multiple data set analysis methods the apportioning of profile intensity to various reflections and to the background become more exact, particularly at low *d* spacings in time-of-flight data. Previous work on model compounds such as copper oxide[13] and nickel-doped magnesium oxides[14] show very significant improvements in the accuracy and precision of structural parameters, including site occupancies and thermal factors, on application of the method. In this paper we have studied the structure of $Sc_2(WO_4)_3$, with natural tungsten, ^{186}W and ^{184}W, in the temperature range 50−823 K extracting anisotropic thermal parameters for the bridging oxygen atoms at each temperature. Using this information a better model of the origin of the thermal contraction of $Sc_2(WO_4)_3$ that occurs on heating is apparent in terms of differences in the behavior at the various bridging oxygen positions.

Experimental Section

Samples of $Sc_2(WO_4)_3$ were synthesized using the method described by Evans et al.[1] Stoichiometric quantities of predried Sc_2O_3 (Aldrich, 99.9%) and either WO_3 (Aldrich, 99.9%), $^{184}WO_3$ (Trace International, 97%) or $^{186}WO_3$ (Trace International, 97.5%) were thoroughly ground under acetone and then repeatedly fired at 1100 °C, with intermediate regrinding, until the powder X-ray diffraction pattern, collected using a Siemens D5000 (Cu Kα $\lambda = 1.54056$ Å) operating in reflection geometry, remained unchanged. Because of the expense of the isotopes, the samples were synthesized at the 400 mg level; to ensure similar counting statistics for each data set, the three isotopic materials were produced and studied in identical quantities.

Neutron diffraction data were collected on the POLARIS high flux, medium resolution diffractometer operating on ISIS. Data collection times for each sample at each temperature corresponded to 225 μA h, about 80 min. For temperatures between 50 K and room temperature (298 K) a closed cycle refrigeration unit (CCR) was used to cool the sample and for temperatures above 298 K data were collected in a RAL furnace. Data were obtained from all three samples at 15 temperatures between 50 and 823 K and each sample was exposed to identical heating and cooling regimes.

Data analysis was undertaken using the GSAS refinement suite.[15] The structural model was taken from Evans et al.[1] For each temperature the three relevant data sets were read into the package as three histograms; atomic coordinates were entered as identical for the modeling of each histogram with the exception of the tungsten scattering length which was taken for the three histograms as ^{184}W, ^{186}W and natural W, +7.30, −0.52 and 4.77 fm, respectively. All data sets were corrected for the effects of absorption, which is significant for ^{186}W. Initial stages of the refinements used isotropic thermal factors for all atoms but these were converted to anisotropic values and refined for all oxygen atoms in the later stages of the refinement. Thermal factors for the scandium and tungsten atoms were maintained as isotropic due to the close to cubic symmetry of the sites adopted by these ions.

In all cases the refinements converged satisfactorily producing excellent profile fits to each of the three histograms contributing to the data, Figure 2. Data collected using the CCR on POLARIS, which produces very low backgrounds, were of higher quality than those collected in the RAL furnace. This was reflected in the precision of the derived positional and thermal parameters and extracted bond lengths and angles in that the low-temperature data produced esds about 2 to 3 times lower than the high-temperature data. To allow comparison between different sites and between temperatures, the anisotropic thermal parameters were diagonalized. In each case the orientation of the thermal ellipsoid is as expected, see Figure 3, with its major axes perpendicular to the Sc−O−W linkages. Figure 2 show the fits obtained to the three 50 K data sets. Table 1 provides an example of the refined atomic positions, thermal parameters and associated errors from the 50 K data. Data from the other temperatures will be deposited.

Results

The main purpose of this study was to allow extraction of thermal parameters for the various oxygen sites and to correlate these with the differences in oxygen site's local environments. Variations in lattice parameters and the cell volume were directly in line with those reported previously by Evans et al.[1] showing a value of -8.27×10^{-5} Å/K for *a*, 1.04×10^{-4} Å/K for *b*, -8.14×10^{-5} Å/K for *c* and −0.0104 Å^3/K for V. Significant improvement in the precision of the extracted positional parameters occurred as a result of the multiisotope multiple dataset methods used—particularly for the data collected in the CCR. Typical errors in the derived coordinates were a factor of 2 lower and those in thermal parameters a factor of 3 lower than those reported previously for unconstrained refinement.[1] This is

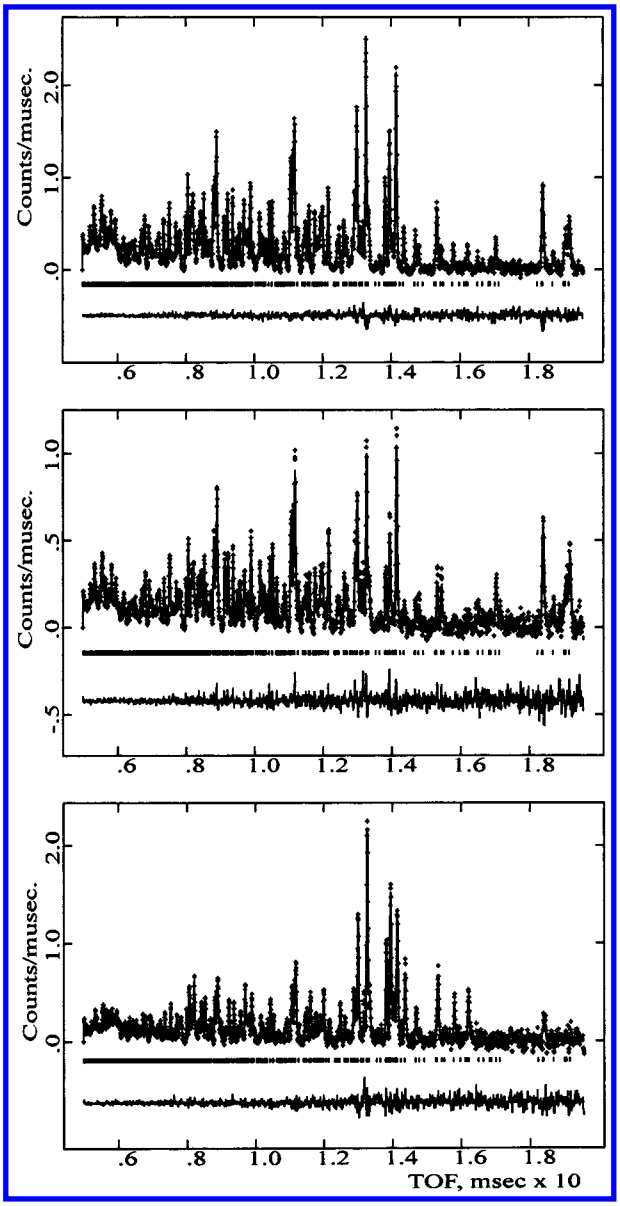

Figure 2. Profile fits obtained using multihistogram analysis to the powder neutron diffraction data from $Sc_2(WO_4)_3$ at 50 K. The upper diagram is natural $Sc_2(WO_4)_3$, center, $Sc_2(^{184}WO_4)_3$, and lower, $Sc_2(^{186}WO_4)_3$. TOF may be converted to *d* spacing (Å) by dividing by 6166.

despite a data collection time per temperature of 240 min in total for three samples, significantly less that used on the much larger sample previously. In addition, the temperature range studied has now been increased up to 823 K.

Sc−O−W Bond Angles. Figure 4 plots the variation in the six different Sc−O−W angles as a function of temperature. Gross variations are in line with those found previously by Evans with the two large Sc−O−W angles (for O2 and O5) decreasing significantly over the temperature range while the smallest angles Sc−O6−W2 and Sc−O4−W1 both increase monotonically. For all these angles the trends tend to level out at the highest temperatures. The variations in the other two interpolyhedral angles, Sc−O1−W2 and Sc−O3−W2, are much smaller and less well defined but these both seem to increase slightly up to room temperature before contracting marginally but the observed changes in these angles lie within the esds over the full temperature range.

The variations in the metal oxygen distances, which can be refined without the constraints of a rigid body model, are

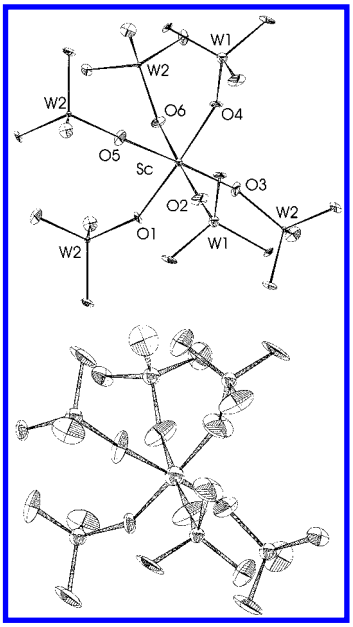

Figure 3. Depiction of a portion of the $Sc_2(WO_4)_3$ structure surrounding a single ScO_6 octahedron at 50 K left and 823 K right. Thermal ellipsoids are shown. For O2 and O5 the short axis of the thermal ellipsoid at 823 K has been reset to a nominal small positive value.

TABLE 1

Refined Atomic Positions for $Sc_2(WO_4)_3$ at 50 K[a]

name	*X*	*Y*	*Z*	$100U_i/U_e$/Å^2
Sc	0.46491(10)	0.38078(7)	0.24943(14)	1.142(20)
W1	0.250000	0.000000	0.47391(32)	0.53(7)
W2	0.11955(22)	0.35586(16)	0.39616(19)	0.47(4)
O1	0.09209(19)	0.14097(16)	0.07928(19)	0.87*
O2	0.12542(22)	0.06158(15)	0.36953(22)	1.17*
O3	0.01234(22)	0.26207(15)	0.32111(23)	1.09*
O4	0.33110(21)	0.40826(15)	0.08179(23)	1.00*
O5	0.07606(20)	0.47387(15)	0.32353(21)	1.04*
O6	0.29639(21)	0.32927(15)	0.36334(22)	1.03*

Thermal Parameters (Å^2) Multiplied by 100.0[b]

name	*U*11	*U*22	*U*33	*U*12	*U*13	*U*23
Sc	1.142(20)	1.14	1.14	0.00	0.00	0.00
W1	0.53(7)	0.53	0.53	0.00	0.00	0.00
W2	0.47(4)	0.47	0.47	0.00	0.00	0.00
O1	0.85(9)	1.65(12)	0.10(9)	−0.09(8)	−0.03(9)	−0.40(9)
O2	0.81(11)	1.73(11)	0.98(12)	0.25(9)	−0.23(8)	−0.01(9)
O3	0.98(12)	1.01(10)	1.27(11)	−0.20(8)	0.03(9)	−0.17(9)
O4	0.60(10)	1.28(11)	1.14(12)	0.30(8)	−0.54(8)	0.27(9)
O5	1.16(10)	0.62(9)	1.35(11)	−0.27(9)	−0.17(8)	0.40(8)
O6	0.58(10)	1.38(12)	1.12(11)	−0.12(8)	0.52(9)	0.07(8)

[a] Space group *Pnca*, $a = 9.69351(10)$, $b = 13.29821(12)$ $c = 9.60118(9)$ Å. Cell volume = 1237.654(21) Å^3. $R_{wp}(Sc_2(WO_4)_3 = 2.62\%$. $R_{wp}(Sc_2(^{186}WO_4)_3 = 3.15\%$. $R_{wp}(Sc_2(^{186}WO_4)_3 = 3.32\%$. [b] Anisotropic thermal factors are defined by $T = \exp\{h^2(a^*)^2u_{11} + ... + 2hk(a^*b^*)u_{12} + ...\}$.

included in Figure 5, together with those corrected for the effects of thermal motion (vide infra). Evans et al.[1] discuss the apparent decrease in Sc−O and W−O in terms of librational type motion of the oxygen atom perpendicular to the M−O direction, Figure 6a; the expected curvature in this motion would be expected to decrease the measured M−O distance. Such corrections are important for molecular species with terminal groups such as C−H and O−H bonds. For framework materials with bridging oxygen atoms, any thermal motion is perpendicular to the M−O direction as shown in Figure 6b and increasing thermal motion of this type would not be expected to cause the same type of decrease in M−O distance as an angular librational mode. The

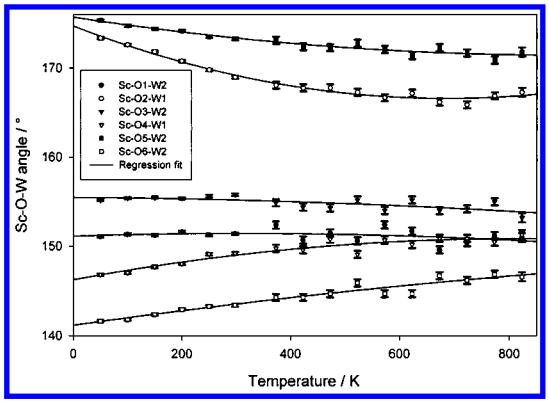

Figure 4. Variations in the Sc−O−W bond angles as a function of temperature. Errors in the angles are plotted at 0.1° for data in the range 50−300 K and 0.3° for data in the range 300−850 K.

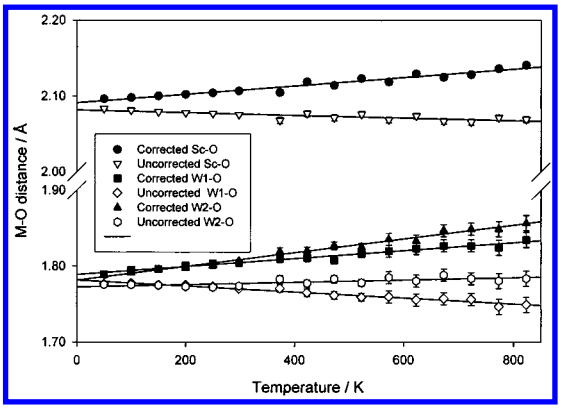

Figure 5. Variation of the average Sc−O and W−O bond lengths as a function of temperature. Uncorrected and corrected distances are shown.

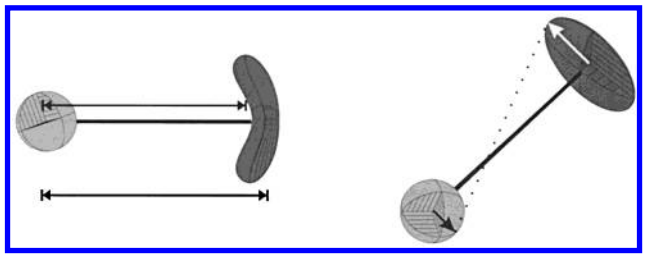

Figure 6. Effects of librational motion (left) and correlated thermal motion (right) in terms reducing the measured interatomic separation with respect to the true separation.

origin of apparently decreasing M−O distances in such cases is in a correlated motion of M and O as previously discussed by Busing and Levy.[16] In such correlated motion of two atoms at the ends of the bond, the effective separation of the two atoms is much larger than the measured average separation and difference between the measured average distance, $d_o = |\langle r_A \rangle - \langle r_B \rangle|$, and the true instantaneous interatomic distance average over time, $d = |\langle r_A - r_B \rangle|$, increases rapidly for large perpendicular components of the thermal motion. Using the expression given by Busing and Levy,[16] derived bond lengths may be corrected for this effect if thermal parameters are known.

Oxygen Thermal Parameters. Full, unconstrained anisotropic refinement of the oxygen atoms was undertaken at each temperature and refinements converged satisfactorily in each case. Values for the thermal parameters extracted for each oxygen site as a function of temperature are summarized in Figure 7a−f. To allow direct comparison, data were diagonalized, but in each case the long axes of the thermal ellipsoids lay almost exactly perpendicular to the Sc−O−W linkages.

The thermal behavior is clearly different for the different oxygen sites and this variation may be correlated with the Sc−O−W angles. Specifically, the open Sc−O−W angles of oxygens O2 and O5 have similar thermal parameter behavior with the magnitude of the ellipsoid axes perpendicular to the Sc−O−W linkages increasing rapidly while the thermal motion along the Sc−O−W linkages actually seems to decrease; for some temperatures a slightly negative value was obtained for this parameter. In contrast, the evolution of the thermal behavior for the other four bridging oxygen atoms is more normal with smooth increases in each of the thermal parameters. In each case the principal axes perpendicular to the Sc−O−W linkages increase most rapidly though for O1 and O3 (with the most "average" Sc−O−W angles) the difference in variation of the three axes is least and the thermal motion closest to isotropic.

The apparent differences in the thermal motions at the various oxygen sites indicates that the polyhedra are not acting as rigid bodies but the vibrational motions involving oxygen are very dependent on the local environment. For the straightest Sc−O−W links along O2 and O5 the thermal motion may be better represented by a mode involving rotation of the oxygen atom around a central position. In terms of the thermal parameters this behavior would fit with the small or negative values obtained for the parallel component of the diagonalized matrix. If the motion was truly a rotation around the midpoint of the polyhedra-join then a toroidal distribution of scattering would be expected; the observed thermal ellipsoid parameters probably represent such a scattering distribution as closely as the structural model permits.

The section of the $Sc_2(WO_4)_3$ structure containing the O2 and O5 bridging oxygen atoms is shown in Figure 8, viewed down each axis direction. Figure 9 is a representation of a local rotational mode between the polyhedra that would produce the observed thermal motion parameters and allow decreases in the measured Sc−O2−W and Sc−O5−W bond angles. The effect of this mode is clearly greatest in the *a* and *c* directions in terms of the separation of W1 and W2, which lies along *c*, and two W2 centers, which lie along *a*. Indeed the W2 −W2 separation, originating the negative thermal expansion in the *a* direction, is 8.065 Å at 50 K decreasing to 7.948 Å at 823 K while the W1−W2 separation decreases from 5.350 to 5.259 Å over the same temperature range. This continuous W2....W1.....W2 linkage is, however, folded up along *b* and the thermal expansion along this direction shows the normal increase with temperature.

The ease of such rotational motions in a portion of the $Sc_2(WO_4)_3$ structure presumably originates in the open Sc−O−W angle and shallow potential well perpendicular to this direction. The more normal thermal behavior of the other bridging oxygen atoms in this material indicate that these sites do not undergo such rotational motions around the Sc−O−W directions to the same extent.

Corrected M−O Distances. As mentioned above, the extracted variation in Sc−O and W−O bond lengths indicate that these distances seemingly remain unchanged or even decrease as the sample temperature increases, while simple considerations of isotropic thermal motion demonstrate that bond lengths should increase with temperature. As discussed above, the origin of a perceived decrease in bond lengths in many materials is in librational motion or in correlated motions. The correction for the effects of correlated thermal motion described by Busing and Levy[16] been applied to the scandium to oxygen and tungsten to oxygen distances in $Sc_2(WO_4)_3$; these corrections

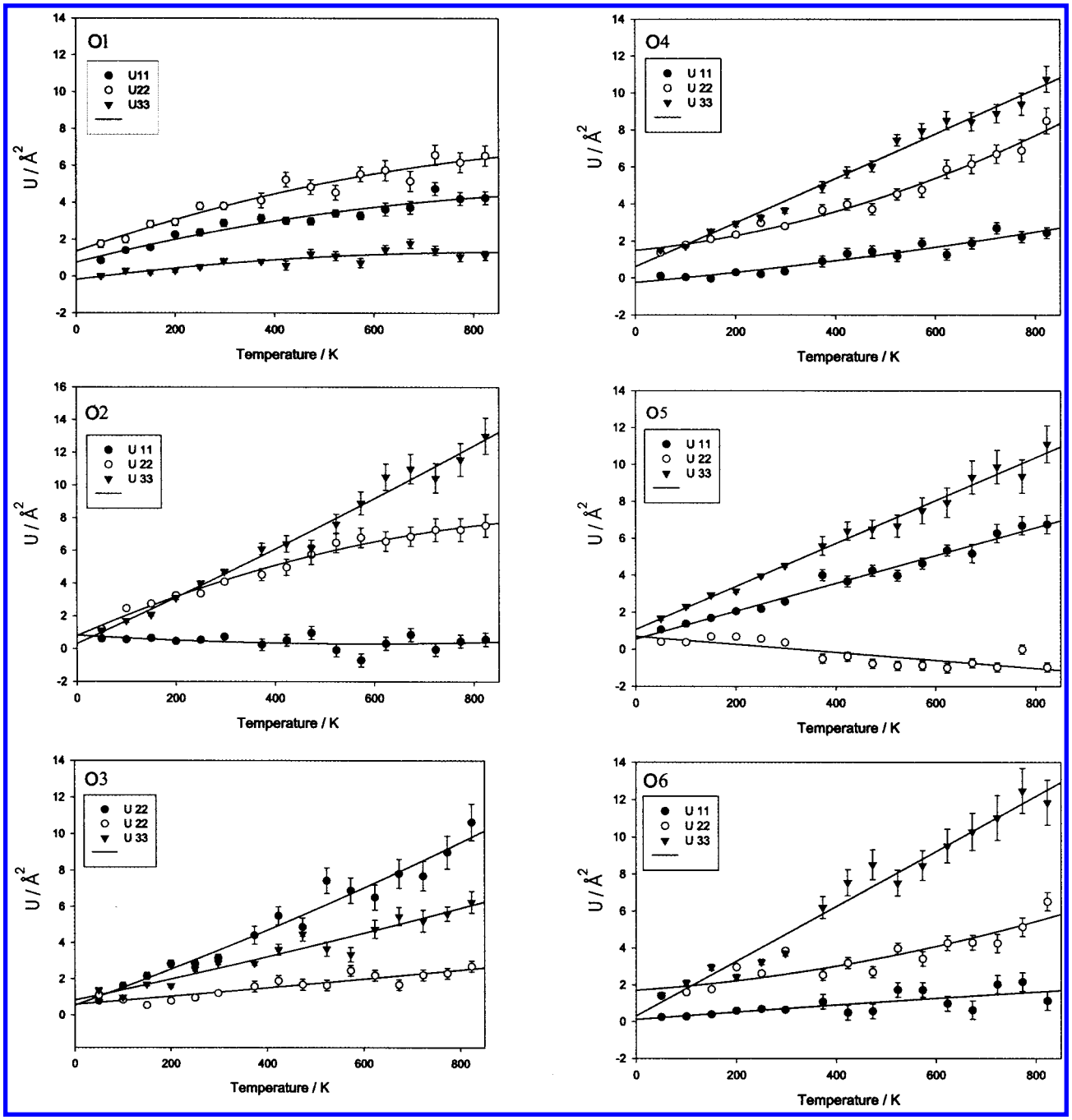

Figure 7. Variations in the diagonalized anisotropic thermal parameters for the bridging oxygen atoms of $Sc_2(WO_4)_3$.

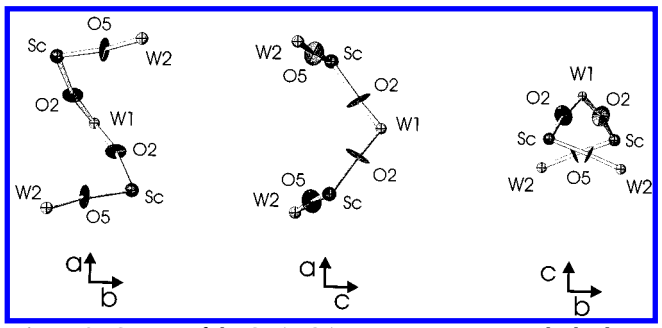

Figure 8. Section of the $Sc_2(WO_4)_3$ structure containing the bridging oxygen atoms O2 and O5 viewed down the three orthogonal directions. Thermal ellipsoids are taken from the 823 K data.

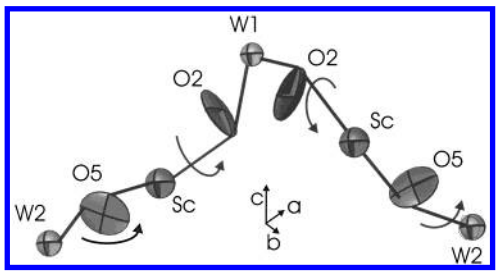

Figure 9. Section of the $Sc_2(WO_4)_3$ structure containing the bridging oxygen atoms O2 and O5 showing a likely local rotational motion involving the bridging oxygen atoms.

only give an upper and lower bound for the corrected distances and in this work data have been corrected by a value corresponding to the average of these two distances. Data in Figure 5 show the corrected average M−O distances within each of the three polyhedra in comparison with the directly extracted distances. A smooth increase in the size of each polyhedron is seen over the temperature range 50−823 K.

Conclusions

Negative thermal expansion in materials such as $Sc_2(WO_4)_3$ and ZrW_2O_8 has previously been described theoretically using rigid unit modes and experimentally using rigid body units. Full analysis of the thermal motion of the oxygen atom in $Sc_2(WO_4)_3$ show that representation in a crystallographic model as totally rigid units involved in librational motion is an approximation and fails to show that transverse vibrational (rocking) or rotational motion in the sections of the structure with open Sc−O−W bridges are the main driver of the NTE effects; for Sc−O−W bridges with more acute angles these local modes are seemingly much weaker and do not contribute to the NTE. A better description of these materials lies with quasi- rigid unit modes, which in structural analysis requires a less constrained model for the thermal motion.

Acknowledgment. We thank the EPSRC for a grant in support of this work and the provision of neutron beam facilities. We also thank R. I. Smith for help with the data collection.

Supporting Information Available: Tables of structure data. This information is available free of charge via the Internet at http://pubs.acs.org.

References and Notes

(1) Evans, J. S. O.; Mary, T. A.; Sleight, A. W. *J. Solid State Chem.* **1998**, *137*, 148.

(2) Woodcock, D. A.; Lightfoot, P.; Ritter, C. *J. Solid State Chem.* **2000**, *149*, 92.

(3) Mary, T. A.; Evans, J. S. O.; Sleight, A. W. *Science* **1996**, *272*, 90.

(4) Taylor, D. *Br. Ceram. Trans. J.* **1984**, *83*, 129.

(5) Dove, M. T. *Phase Transitions* **1997**, *61*, 1.

(6) Woodcock, D. A.; Lightfoot, P.; Ritter, C. *Chem. Commun*. **1998**, 107.

(7) Amos, T. G.; Yokochi, A.; Sleight, A. W. *J. Solid State Chem*. **1998**, *14*, 303.

(8) Attfield, M. P.; Sleight, A. W. *Chem. Mater*. **1999**, *9*, 349.

(9) Evans, J. S. O. *J. Chem. Soc*., *Dalton Trans*. **1999**, 3317.

(10) Pryde, A. K. A.; Hammonds, K. D.; Dove, M. T.; Heine, V.; Gale, J. D.; Warren, M. C. *J. Phys.: Condens. Matter*. **1996**, *8*, 10973.

(11) Forster, P. M.; Yokochi, A.; Sleight, A. W. *J Solid State Chem*. **1998**, *140*, 159.

(12) Forster, P. M.; Sleight, A. W. *J. Inorg. Mater*. **1999**, *1*, 123.

(13) Henry, P. F.; Weller, M. T.; Wilson, C. C. Submitted to *J Appl. Crystallogr*.

(14) Henry, P. F.; Weller, M. T.; Wilson, C. C. Submitted to *J. Appl. Crystallogr*.

(15) Larson, A. C.; Von Dreele, R. B. *Generalised Structure Analysis System*; Los Alamos National Laboratory: Los Alamos, NM, 1994.

(16) Busing, W. R.; Levy H. A. *Acta Crystallogr.* **1964**, *17*, 142.